Engineering Fracture Mechanics 200 (2018) 50–63

Contents lists available at ScienceDirect

Engineering Fracture Mechanics

journal homepage: www.elsevier.com/locate/engfracmech

Probabilistic assessment of creep-fatigue crack propagation in austenitic stainless steel cracked plates

A. Vojdani[a], G.H. Farrahi[a,*], A. Mehmanparast[b], B. Wang[c]

[a] School of Mechanical Engineering, Sharif University of Technology, Tehran, Iran
[b] Offshore Renewable Energy Engineering Centre, Cranfield University, Cranfield, UK
[c] Department of Mechanical, Aerospace & Civil Engineering, Brunel University London, Uxbridge, UK

ARTICLE INFO

Keywords:
Creep-fatigue
Crack growth
Probabilistic assessment
Uncertainty

ABSTRACT

This study investigates the effects of uncertainties in the prediction of creep-fatigue crack propagation in 316L(N) austenitic stainless steel plates containing a semi-elliptical surface defect. Different parameters in geometry, material behavior and test condition are considered as random variables in probabilistic assessments. Monte-Carlo sampling method is employed to estimate the probability distribution of desired outputs such as propagated crack sizes, stress intensity factors and creep rupture life. It is shown that, the standard deviation of the predicted crack sizes in both through-wall direction and along the surface of the plate will be increased by increasing the time (hence the crack size). It is observed also that, the uncertainty in the prediction of the half-surface crack lengths, c_i, is significantly more than that of crack depths, a_i. Furthermore, probabilistic evaluations are performed using different reliability methods to calculate the probabilities of exceedance of available experimental results. These evaluations clarified the importance of consideration of uncertainties in creep-fatigue crack growth prediction. Sensitivity analyses are carried out to provide useful information about the order of importance of random variables associated to the different limit state functions. It is found that, the CoV (Coefficient of Variation) of the initial crack size, a_0 and c_0/a_0 has a significant role on the importance of these parameters; and therefore they may be important random variables in such probabilistic assessments, based on their CoV and defined limit state functions.

1. Introduction

For defective components, which operate under the combination of static and cyclic loading at elevated temperatures, an assessment of creep-fatigue crack growth may be necessary in order to demonstrate the integrity of these components. Various deterministic studies carried out to investigate the behavior of creep-fatigue crack propagation [1–6]. Li et al. [1] employed the Cohesive Zone Model (CZM) to numerically simulate the crack growth. A trinomial superposition model has been proposed by Liu et al. [2] to predict creep-fatigue crack growth rates. Mehmanparast et al. analyzed the creep and creep-fatigue crack growth results for a range of steels taken from the HIDA collaborative project, and identified the interactive creep-fatigue behavior of these steels. They used ASTM E2760-10 creep-fatigue crack growth testing standard, as guideline to analyze the results [3]. A presentation has been published by Nikbin [4] about testing, modeling and component life assessment of welds under creep-fatigue crack growth condition. Saxena [5] presented the progress made in the field of time-dependent fracture mechanics. A creep-fatigue interaction

* Corresponding author.
E-mail address: farrahi@sharif.edu (G.H. Farrahi).

https://doi.org/10.1016/j.engfracmech.2018.07.022
Received 26 April 2018; Received in revised form 8 July 2018; Accepted 13 July 2018
Available online 20 July 2018

damage model has been proposed by Xu et al. [6] in order to evaluate damage evolution and crack growth behavior in creep-fatigue regime. Although these studies provide valuable information, they do not address the issue of the effect of uncertainties on the response of defective components. In reality, there are different sources of uncertainty in the areas of "material behavior", "operating (test) conditions", "geometry parameters", "evaluation models" and "inspection methods and data", which considering them in probabilistic assessments leads to a more comprehensive understanding of the remaining life of a cracked component.

Probabilistic investigations and reliability analysis of creep-fatigue behavior, have been performed by other researchers on either crack initiation (damage accumulation) or crack growth. Mao and Mahadevan [7] proposed a probabilistic approach for creep-fatigue reliability analysis, which consists of a failure function that models the effects of creep-fatigue interaction without symmetry assumptions. Uncertainties in creep and fatigue life, creep and fatigue loading cycles, and limitation of test data are included in this study. A method has been outlined by Harlow and Delph [8] in order to incorporate the scatter bands in fatigue cycles-to-failure and creep rupture times-to-failure into a probabilistic creep-fatigue failure model. Their study has been conducted in the context of the well-known damage fraction summation rule for creep and fatigue damage. Probabilistic life models have been derived by Ibisoglu and Modarres [9] based on the creep rupture behavior of 316FR austenitic stainless steel. A standard Bayesian regression approach was used to estimate the parameters of the proposed creep-fatigue model. Hu et al. [10] conducted experimental study on a nickel-based super alloy in order to investigate the effects of dwell times on the creep-fatigue behavior. Also, they established a probabilistic model based on the applied mechanical work density (AMWD) method, to describe the scattering in creep-fatigue life-times.

Relatively few studies performed on statistical and probabilistic assessment of creep-fatigue crack growth. A study reported by Dogan et al. [11] has been focused on the life assessment approaches and the sources of scatter in creep-fatigue crack growth data. Different sources of scatter due to test equipment, testing procedures, data analysis method and creep-fatigue interaction, are explained in this work. Furthermore, they describe sensitivity analysis of high-temperature crack growth data, including probabilistic and deterministic methods. Probabilistic analysis of crack growth, based on the damage accumulation mechanisms have been done in the research of Wei et al. [12]. In this paper, a deterministic creep-fatigue accumulation model has been developed, and Monte-Carlo simulation method is used to investigate the probabilistic behavior of the derived deterministic model. In the study performed by Wei et al. [13], a linear superposition theory is proposed to model the creep-fatigue-oxidation crack growth. Monte-Carlo simulation has been implemented into creep-fatigue-oxidation model, by introducing the uncertainties of parameters in creep, fatigue and oxidation crack growth laws.

Several experimental and deterministic investigations have been carried out to describe the behavior of semi-elliptical defect in austenitic stainless steel plates subjected to creep-fatigue loading condition [14–20]. Although, deterministic studies provide worthy information about the creep-fatigue crack propagation in the cracked plates, they do not address the effects of the indeterminacy of the various input parameters, on the prediction of creep-fatigue crack growth. The present study evaluates the probabilistic behavior of such specimens, considering the sources of uncertainty in "test condition", "material behavior", and "geometry parameters". The areas covered in this study are as follows:

I. *Estimation of probability distribution of the results:* in this phase, Monte-Carlo sampling method has been applied in order to estimate the probability distribution of desired outputs, i.e. propagated crack sizes, initial and final stress intensity factors, and creep rupture life.
II. *Calculation of probabilities of exceedance of experimental results:* in the second phase, probabilistic assessments have been performed in conjunction with experimental results [20] utilizing different reliability methods (e.g. FORM, Sampling, etc.). Assessments have been carried out with two aims: first, for understanding the influence of uncertainties on the creep-fatigue crack growth prediction, in comparison with available experimental data; and second, for investigating the importance of random variables corresponding to each of the defined limit state functions.
III. *Sensitivity analysis:* in the last phase, the order of importance of the random variables corresponds to the different limit state functions have been extracted as a by-product of the previously performed FORM analysis. The γ importance vector has been used to investigate the relative importance of the random variables.

2. Deterministic assessment

Probabilistic investigations in present study have been implemented on a benchmark problem, which its experimental background is reported by Poussard and Moulin [20] (see Section 2.1). It should be noted that deterministic calculations are at the heart of the probabilistic assessments. The deterministic approach used in the present study for prediction of the creep-fatigue crack propagation of the benchmark problem, is adapted from the procedures employed by Baker et al. [14], based on the R5, Volume 4/5 procedure [21] (see Section 2.2).

2.1. Overview of experiment

The benchmark problem consists of a 316 L(N) austenitic stainless steel plate containing a semi-elliptical surface crack, subjected to a set of fatigue and creep-fatigue loadings at 650 °C [20]. Plate geometry, test configuration, and location of the defect are shown in Fig. 1. The plate has a thickness of $t = 24.5$ mm, and a width of $w = 350$ mm, loaded through an arm with a length of $l = 350$ mm. Initial surface crack of depth, $a_0 = 7.9$ mm and width, $2c_0 = 87.2$ mm, is achieved after high temperature fatigue pre-cracking (Fig. 2).

Loading conditions, along with the experimental results are summarized in Table 1. Creep-fatigue cycles consist of a dwell of one

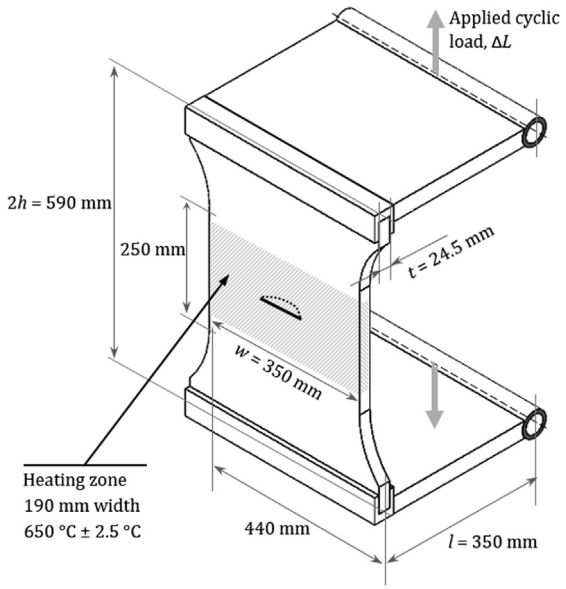

Fig. 1. Geometry and test configuration (adapted from [20]).

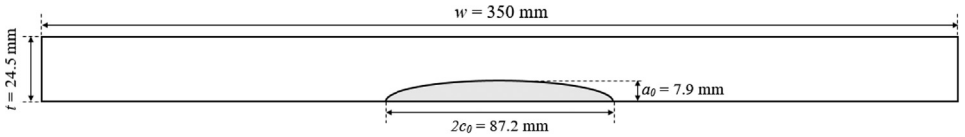

Fig. 2. Shape and dimension of initial semi-elliptical defect.

Table 1
Loading history and experimental crack growth results [20].

Loading sequence	Number of cycles	Cumulative creep-fatigue cycles	Max. load (kN)	Min. load (kN)	Exp. crack depth a (mm)	Exp. crack surface $2c$ (mm)
Fatigue pre-cracking at 650 °C	68,271	–	−13.5	3.5	7.9	87.2
1st creep-fatigue loading	474	474	−14	14	8.75	89.05
1st fatigue loading	2100	–	−10	10	9.2	90.35
2nd creep-fatigue loading	781	1255	−14	14	10.35	92.9
2nd fatigue loading	1500	–	−10	10	10.85	94.45
3rd creep-fatigue loading	1356	2611	−14	14	12.65	103.15
3rd fatigue loading	1200	–	−10	10	12.75	106.45
4th creep-fatigue loading	518	3129	−14	14	13.35	109.95
Fatigue post cracking at room temperature	8578	–	–	–	–	–

hour at the maximum load (−14 KN) of each cycle. Note that the setup of the experiment was such that applying a negative (compressive) load would result in a primary positive bending stress and secondary negative membrane stress on the cracked side of the plate.

2.2. Deterministic assessment procedure

Several deterministic evaluations performed to predict the behavior of creep-fatigue crack growth in semi-elliptical cracked plates [14–19]. A16 [22], R5 [21] and JNC [23] procedures may be used to investigate creep-fatigue crack growth in defective components. As noted earlier, deterministic assessment in present study is adapted from an approach utilized by Baker et al. [14] based on the R5, Volume 4/5 procedure [21]. The employed approach is summarized below.

2.2.1. Input parameters and desired outputs

The input parameters required for calculations are as follows:

Table 2
Material properties.

	Related equation	Ref.	Parameters		
Fatigue crack growth	(2)	[14,18]	C_f	m	
			4.662×10^{-7}	2.339	
Creep crack growth	(7)	[18]	A	q	
			1.117×10^{-2}	0.673	
Creep strain	(10)	[14,18,21]	C_1	C_2	C
			5.863×10^{-11}	0.565	1.018×10^{-25}
			n_1	n	
			4.233	9.407	

- Geometry parameters consist of plate dimensions, arm length, and initial crack size (see Section 2.1)
- Test condition, involving temperature, creep dwell time, and loading configurations (see Section 2.1)
- Various material properties of 316 L(N) austenitic stainless steel, which represented in Table 2.

The desired outputs of deterministic calculations in present study are:

- Estimation of the crack depth (a) and crack surface size (c) after each four creep-fatigue loading (Table 1)
- Estimation of creep rupture life at the end of the last creep-fatigue loading

2.2.2. Creep-fatigue crack growth calculations

Selection of an appropriate method to evaluate the creep-fatigue crack growth rate, depends on the cyclic plastic zone size at the surface of the component and current crack length [21]. In this study (based on the [14]), a simple sum of the contributions due to creep and fatigue crack growth rates, has been used to calculate the total crack growth rate.

$$\frac{da}{dN} = \left(\frac{da}{dN}\right)_f + \left(\frac{da}{dN}\right)_{cr} \tag{1}$$

where a is the crack depth and N is the number of cycles. Subscripts "f" and "cr" represent the fatigue and creep terms, respectively. For half-surface crack length (c) a similar equation has been used. The contribution of each part (creep and fatigue) can be determined as follows.

2.2.2.1. Fatigue crack growth. The rate of fatigue crack growth is given by,

$$\left(\frac{da}{dN}\right)_f = C_f(\Delta K_{eff})^m \tag{2}$$

where material constants C_f and m are temperature dependent and are obtained from Table 2, in which, da/dN is in (mm/cycle) and ΔK_{eff} is in (MPa m$^{1/2}$). ΔK_{eff} is effective stress intensity factor range that is related to the total stress intensity factor range, ΔK.

$$\Delta K_{eff} = q_0 \Delta K \tag{3}$$

where,

$$\Delta K = K_{max} - K_{min} \tag{4}$$

and

$$q_0 = 1,\ R \geqslant 0;$$
$$q_0 = (1-0.5R)/(1-R),\ R < 0 \tag{5}$$

In above equations, $R = K_{min}/K_{max}$, and K_{max} and K_{min} are the maximum and minimum stress intensity factors during a loading cycle, respectively. Stress intensity factors at crack depth, a, and crack surface, c, are calculated based on the solutions derived by Newman and Raju [24], for a semi-elliptical surface defect in a finite width plate under bending and tension. The parameter q_0, is the fraction of the total load range for which a crack is judged to be open [21]. In the present work in which $R = -1$, crack closure parameter, q_0, is obtained from Eq. (5) for crack depth. However, this parameter is considered equal to unity for crack surface, according to the justification explained by Baker et al. [14].

2.2.2.2. Creep crack growth. Creep crack growth per cycle, is calculated by the following equation.

$$\left(\frac{da}{dN}\right)_{cr} = \int_0^{t_{dwell}} \dot{a}_{cr}\, dt \tag{6}$$

where t_{dwell} is the creep dwell time per cycle, and $\dot{a}_{cr}$ is the creep crack growth rate that is given by [14]:

$$\dot{a}_{cr} = 2A(C^*)^q, \quad t < t_{red};$$
$$\dot{a}_{cr} = A(C^*)^q, \quad t \geqslant t_{red} \tag{7}$$

where material and temperature dependent parameters, A and q are obtained from Table 2, in which, $\dot{a}_{cr}$ is in (mm/h) and C^* is in (N/mm/h). t_{red} is redistribution time that can be determined from [14,21]. The parameter C^* characterizes the crack tip stress and strain rate fields, for steady state creep conditions. This is the creep equivalent of the J-contour integral used to describe elastic-plastic fracture [25]. C^* parameter may be expressed in terms of reference stress, σ_{ref}, creep strain rate at the current reference stress, $\dot{\varepsilon}^{cr}_{ref}$ and characteristic length, R', as:

$$C^* = \sigma_{ref}\dot{\varepsilon}^{cr}_{ref}R' \tag{8}$$

where parameter R' is defined as follows.

$$R' = \left(\frac{K}{\sigma_{ref}}\right)^2 \tag{9}$$

In above equation, K is stress intensity factor. Creep deformation behavior follows the equation given by,

$$\varepsilon_{cr} = F_d(C_1 t^{C_2}\sigma^{n_1}), \quad t \leqslant t_{fp}; \quad \text{(Primary creep)}$$
$$\varepsilon_{cr} = F_d[C_1 t_{fp}^{C_2}\sigma^{n_1} + 100C\sigma^n(t-t_{fp})], \quad t > t_{fp} \quad \text{(Secondary creep)} \tag{10}$$

where C, C_1, C_2, n and n_1 are temperature dependent constants that given in Table 2. In Eq. (10), t is time in hours, σ is the applied stress in MPa, and ε_{cr} is the percentage of creep strain. Parameter, F_d, is a scaling factor with a value of unity. This parameter will be considered as a random variable in next section, in order to address the uncertainty in the creep strain parameter. t_{fp} is primary-secondary transient time that can be obtained by equating the rates of above equations.

$$t_{fp} = \left[\frac{100C}{C_1C_2}\sigma^{n-n_1}\right]^{\frac{1}{C_2-1}} \tag{11}$$

The solution developed by Goodall and Webster [26] has been used to determine the reference stress. Defining geometry parameters $\alpha = a/t$ and $\gamma = 2ac/wt$, the reference stress is given by,

$$\sigma_{ref} = \frac{(\sigma_b + 3\gamma\sigma_m) + \{(\sigma_b + 3\gamma\sigma_m)^2 + 9\sigma_m^2[(1-\gamma)^2 + 2\gamma(\alpha-\gamma)]\}^{0.5}}{3\{(1-\gamma)^2 + 2\gamma(\alpha-\gamma)\}} \tag{12}$$

where σ_b and σ_m are the bending stress and the membrane stress, respectively. These stresses with opposite signs that are considered in the present study (i.e. one positive and one negative), are defined as

$$\sigma_m = \frac{L}{wt} \tag{13}$$

$$\sigma_b = \frac{-3Ll}{2w\left(\frac{t}{2}\right)^2} \tag{14}$$

where L is the applied load and w, t and l are geometry parameters that defined in Section 2.1. Note that a negative load leads to a positive bending stress and vice versa (see Fig. 1). For deep crack where $a/t > (1 + \sigma_m/\sigma_{ref})/(2 - 2c/w)$, an extended expression of reference stress is used by Baker et al. [14]. However, preliminary deterministic and probabilistic assessments showed that this extension of reference stress equation for deep cracks, had no significant effect on the results of this study and therefore it is not employed here.

Creep rupture time is considered as follows [21].

$$t_r = 10^{\left(13.72 - \frac{[\sigma+353.1][\theta-227]}{21.13\times10^3}\right)} \tag{15}$$

where t_r is the rupture life in hours, σ is the applied stress in MPa and θ is the temperature in °C.

2.2.3. Deterministic results

Based on the procedure described earlier, estimations of crack growth in the through-wall direction, a, and along the surface of the plate, c, as a function of time are shown in Figs. 3 and 4, respectively. The crack growth increments due to the pure fatigue loading (benchmarking) during the test are shown by step changes in these figures. The time-dependent crack growth trends were occurred as a result of the creep-fatigue loading condition during the test.

3. Probabilistic assessment

3.1. Sources of uncertainty

The uncertainties considered in the current research can be distinguished in the following categories,

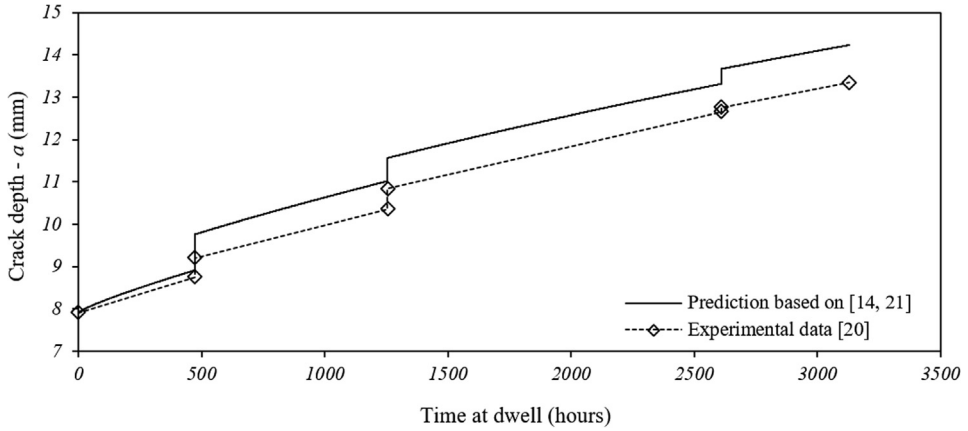

Fig. 3. Deterministic calculated crack depth, a, in comparison with experimental results.

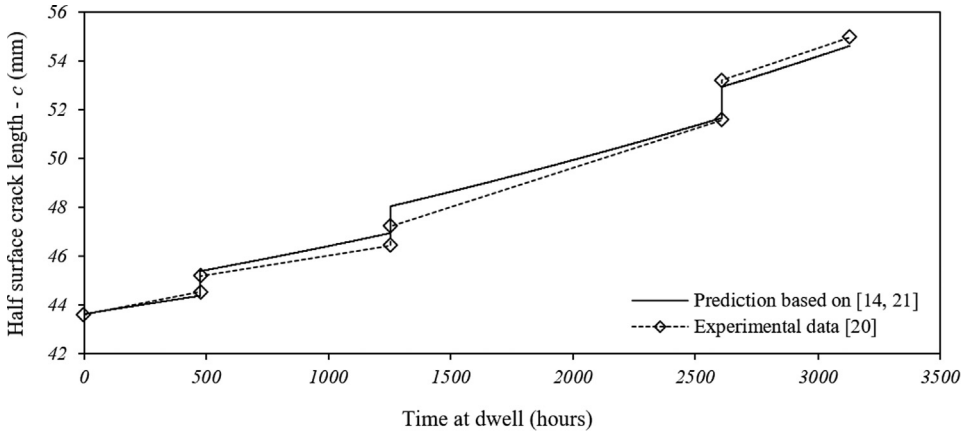

Fig. 4. Deterministic calculated half-surface crack length, c, in comparison with experimental results.

- Material behavior
- Geometry parameters
- Test condition

Random variables that represent the uncertainties in "material behavior", consist of fatigue crack growth equation parameter, C_f (Eq. (2)), creep crack growth rate equation parameter, A (Eq. (7)), and scaling factor, F_d, with mean value of unity, which is a multiplication factor in both primary and secondary creep strain relationships (Eq. (10)). It should be noted that, there is a negative correlation between creep strain rate scaling factor, F_d, and constant A in creep crack growth rate equation [21]. Therefore, a correlation factor of -0.5 has been assumed between these two parameters.

Uncertainties in "geometry parameters" include the thickness, t, and width, w, of the plate, arm length, l, initial crack depth, a_0, and initial crack aspect ratio, c_0/a_0. Generally, uncertainty in initial crack size is an important issue, which has been discussed in the literature [25,27,28].

Various random variables, i.e. Maximum load in pure fatigue cycles, L_f, Maximum load in creep-fatigue cycles, L_{cf}, number of cycles, minimum to maximum load ratios, R_f and R_{cf}, test temperature, θ, and creep dwell time, t_{dwell}, indicate the uncertainties in "test condition". It should be noted that, in the present study, the uncertainties in "test condition", are considered as unique values for the entire test, not for each cycle, individually.

The probability distribution of random variables are given in Table 3. Coefficient of Variation (CoV) that represents the extent of variability in relation to the mean may be an important measure in a probabilistic assessment. In this work, the CoV (i.e. std/|mean|) of parameters A, F_d, a_0 and t are adapted from [29], and the CoV of parameter C_f, is estimated based on [30]. It is noted that, for similar conditions it is expected that a larger mean of initial crack size leads to a lower CoV of this parameter, assuming a relatively constant standard deviation of crack detection. However, the considered CoV for parameters a_0 and c_0/a_0 in present work, is similar to the value assumed in [29], for smaller and different initial crack. For the other parameters, the CoV has been assumed. Mean value of the random variables are assumed equal to quantities employed in the deterministic approach (section 2).

Table 3
Probability distribution of random variables.

Random variable	Symbol	Distribution	Mean	CoV
Material behavior				
Creep crack eq. factor	A	Log-normal	1.117e − 2	0.5
Creep deformation scaling factor	F_d	Log-normal	1	1.3
Fatigue crack eq. factor	C_f	Log-normal	4.662e − 7	0.3
Geometry parameters				
Initial crack depth	a_0	Log-normal	7.9 mm	0.2
Initial aspect ratio	c_0/a_0	Log-normal	5.519	0.2
Arm length	l	Log-normal	350 mm	0.015
Plate thickness	t	Log-normal	24.5 mm	0.025
Plate width	w	Log-normal	350 mm	0.025
Test condition				
Maximum load (creep-fatigue)	L_{cf}	Normal	14 KN	0.015
Maximum load (fatigue)	L_f	Normal	10 KN	0.015
Number of cycles at i^{th} creep-fatigue loading (i = 1–4)	–	Log-normal	Table 1	0.05
Number of cycles at j^{th} fatigue loading (j = 1–3)	–	Log-normal	Table 1	0.05
Load ratio (creep-fatigue)	R_{cf}	Normal	−1	0.01
Load ratio (fatigue)	R_f	Normal	−1	0.01
Creep hold time	t_{dwell}	Log-normal	1 h	0.03
Temperature	θ	Normal	650 °C	0.01

3.2. Probabilistic assessment procedure

Probabilistic assessments have been carried out in the following two areas:

Case A. Estimation of probability distribution of the outputs, consisting of crack depth, a, and half-surface crack length, c, after each four creep-fatigue loadings (see Table 1), initial and final stress intensity factors, and final creep rupture life; using Monte-Carlo sampling method.

Case B. Calculation of probability of exceedance of experimental values reported by Possuard and Moulin [20] (Table 1); using reliability methods (i.e. FORM, Modified FORM, Sampling, etc.). The first purpose of this calculation is to understand the influence of uncertainties on creep-fatigue crack growth prediction, in comparison with available experimental data. In addition, this calculation assists to investigate the importance of random variables corresponding to each of the limit state functions.

The limit state functions used to calculate the probabilities of exceedance of experimental crack sizes, are considered as,

$$g_i^a(\boldsymbol{x}) = a_i^{\exp} - a_i(\boldsymbol{x}) \quad (i = 1 \text{ to } 4) \tag{16}$$

$$g_i^c(\boldsymbol{x}) = c_i^{\exp} - c_i(\boldsymbol{x}) \quad (i = 1 \text{ to } 4) \tag{17}$$

where $a_i^{\exp}$ and $c_i^{\exp}$ are, respectively, the experimental crack depth and half-surface crack length, after i^{th} creep-fatigue loading. $a_i(\boldsymbol{x})$ and $c_i(\boldsymbol{x})$ are i^{th} calculated crack depth and half-surface crack length, respectively, as functions of random variables vector, $\boldsymbol{x}$.

Furthermore, a limit state function for creep rupture life is applied as follows.

$$g^L(\boldsymbol{x}) = life(\boldsymbol{x}) - \text{life}_{cr} \tag{18}$$

where life ($\boldsymbol{x}$) is the creep rupture life calculated from Eq. (15) as a function of random variables vector, $\boldsymbol{x}$. life_{cr} is the critical remaining life that is assumed to be equal to 1.5 years (13,140 h). The critical value may be selected based on the inspection intervals or determined as critical allowable remaining life. Probabilistic assessments are carried out using the *Rt* software, developed by Mahsuli et al. [31].

3.3. Probabilistic results

3.3.1. Case A: Probability distribution of outputs

Probability distribution of crack depths, a_i, and half-surface crack lengths, c_i, after each four creep-fatigue loading (Table 1), which is obtained by Monte-Carlo sampling method, are illustrated in Figs. 5 and 6, respectively. The comparison of probability distribution of the first and the fourth propagated crack size (in both through-wall direction and along the surface of the plate) shows an increased standard deviation and a decreased peak of pdf (probability density function), for larger crack.

It can be observed that, the uncertainty in the prediction of the half-surface crack lengths, c_i, is significantly more than that of crack depths, a_i (Fig. 7). For example, the standard deviation (std) and coefficient of variation (CoV) of final crack depth, a_4, are approximately equal to 2.3 mm and 0.17, respectively; while the final half-surface crack length, c_4, has a std and CoV of approximately 15.6 mm and 0.29, respectively. This may be caused by the fact that the crack growth through the thickness direction and along the plate surface, are significantly affected by the related stress intensity factors at the deepest and surface points, respectively. The pdfs of initial and final stress intensity factors, related to a_0, c_0 and a_4, c_4 are shown in Fig. 8. This figure illustrates that the prediction of surface point's stress intensity factors involves higher uncertainty (more standard deviation) compared to deep point's

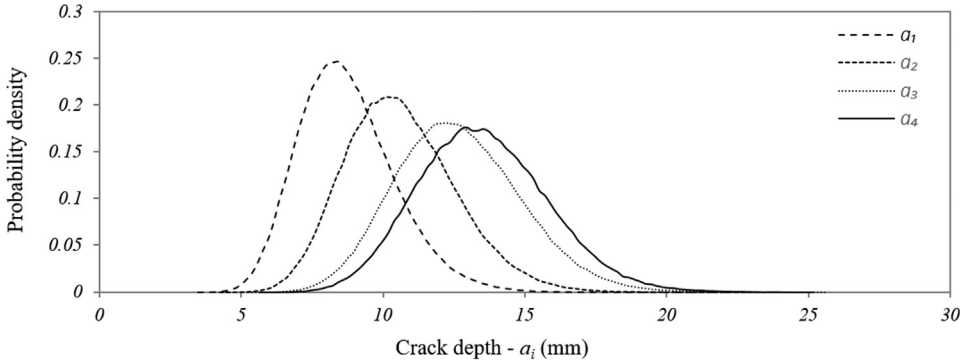

Fig. 5. Probability distribution of crack depths, a_i, after each of four creep-fatigue loading.

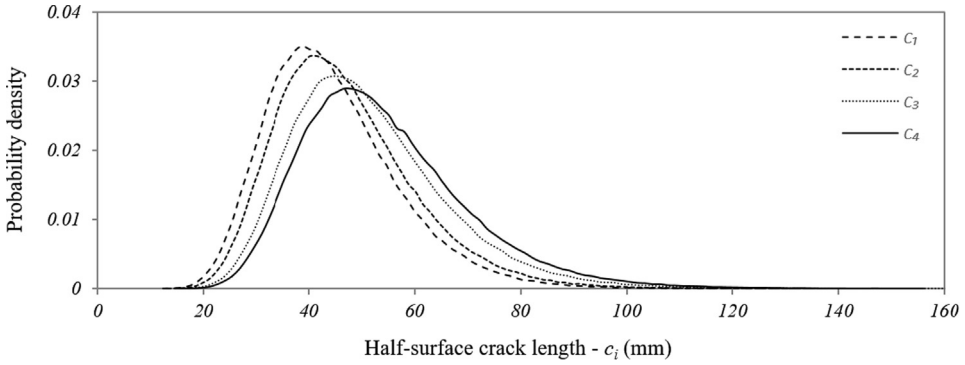

Fig. 6. Probability distribution of half-surface crack lengths, c_i, after each of four creep-fatigue loading.

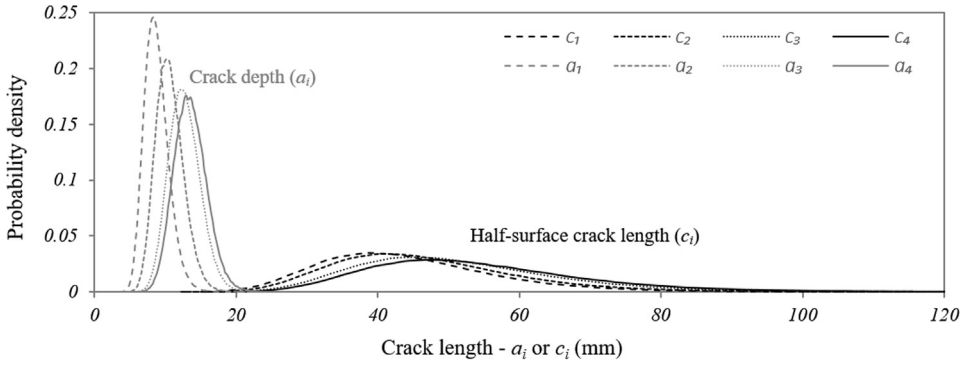

Fig. 7. Comparison of probability distribution of crack depths and half-surface crack lengths.

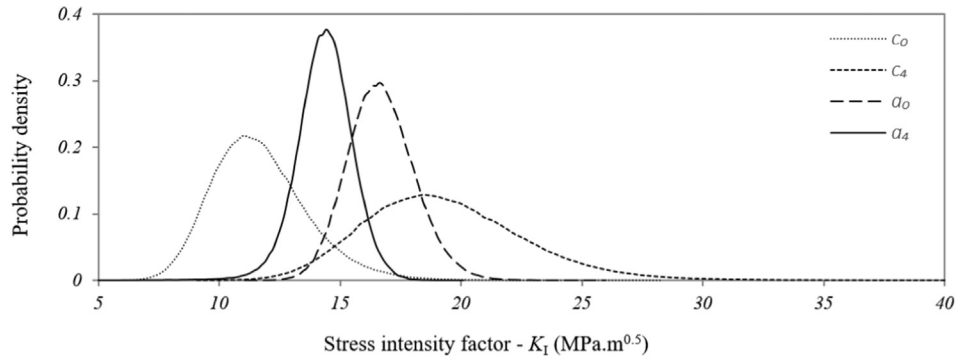

Fig. 8. Probability distribution of initial and final stress intensity factors.

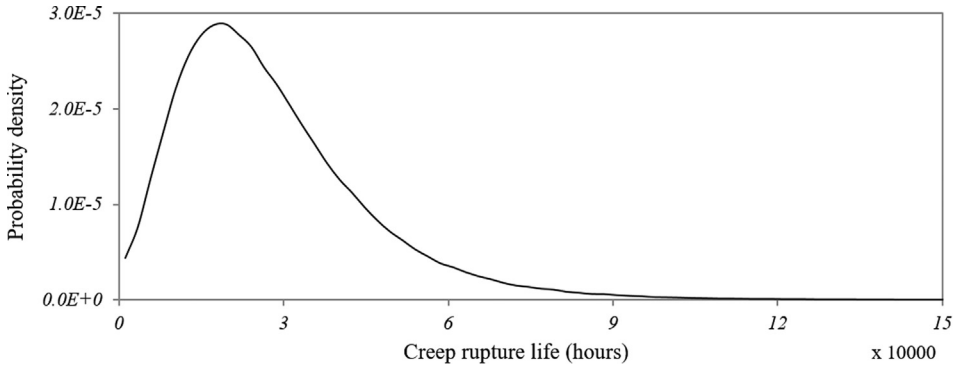

Fig. 9. Probability distribution of creep-rupture life related to the final crack.

stress intensity factors. Also, as the crack grows, the mean and std of stress intensity factors in the through-wall direction (related to a) and along the surface of the plate (related to c) will be decreased and increased, respectively. Fig. 9 demonstrates the pdf of creep rupture life after the last creep-fatigue loading.

The comparison between the experimental, deterministic and probabilistic results, are given in the Table 4. It is found that, there is no significant difference between the mean value of the probabilistic results and deterministic or experimental results. However, probabilistic assessments are accompanied by valuable complementary data (i.e. standard deviation), that indicates the effects of the randomness of the input parameters on the uncertainty of the results. As mentioned earlier, the CoV of the half-surface crack lengths, c_i, are obtained higher than the CoV of the crack depths, a_i. Although, this table shows a relatively high CoV for the final creep rupture life, which represents the important role of the input random variables on the probabilistic prediction of the creep rupture life.

3.3.2. Case B: Calculations of probabilities of exceedance

Cumulative Distribution Function (CDF) of each four-crack depths, a_i, and four-half surface crack lengths, c_i, obtained by Monte-Carlo sampling method, are illustrated in Figs. 10 and 11, respectively. The amount of each CDF at the related experimental values (which showed by vertical lines in these Figs.), can be used to calculate the probabilities of exceedance of the experimental results.

In addition to the above method which is named as *histogram sampling*, different reliability methods, i.e. *FOSM*, *FORM*, *Modified FORM* (named as *MFORM*), *probability sampling* and *importance sampling*, are utilized in order to evaluate the probabilities of failure (PoF), $P(g(\boldsymbol{x}) \leqslant 0)$, associated with the previously defined limit state functions (Eqs. (16)-(18)). Note that, the term "PoF" means the probability of falling in the region where the limit state function, $g(\boldsymbol{x})$, is negative. For limit state functions $g_i^a(\boldsymbol{x})$ and $g_i^c(\boldsymbol{x})$, PoF represents the probability of exceedance of experimental values.

In *Modified FORM* (*MFORM*) approach, first, the last two trial points in the search for the Most Probable Point (MPP) in *FORM*, are used to calculate the first principal curvature, κ_1, of the limit state function. Then the probability of failure that obtained by *FORM*, will be modified according to Breitung's improved formula, in *Rt* software [31].

Probability sampling refers to Monte-Carlo sampling method with a specified target coefficient of variation of failure probability ($\delta_{P_f} = \frac{\sigma_{P_f}}{\mu_{P_f}}$). Sampling continues until the δ_{P_f} reaches its target value. A reasonable amount of $\delta_{P_f} = 0.02$ is considered here. The relationship between the probability of failure, P_f, target coefficient of variation, δ_{P_f}, and the number of samples, N_s, can be gained by,

Table 4
Comparison between the experimental, deterministic and probabilistic results.

Parameter	Experimental results [20]	Deterministic results	Probabilistic results		
			Mean	std	CoV
Crack depth (mm)					
a_1	8.75	8.91	8.73	1.698	0.195
a_2	10.35	11.02	10.62	1.960	0.185
a_3	12.65	13.31	12.68	2.224	0.175
a_4	13.35	14.23	13.52	2.293	0.170
Half-surface crack length (mm)					
c_1	44.53	44.38	44.30	12.59	0.284
c_2	46.45	46.96	46.82	13.17	0.281
c_3	51.58	51.68	51.32	14.61	0.285
c_4	54.98	54.63	54.12	15.60	0.288
Final creep rupture life (hours)					
t_r	–	23658.8	27814.9	17480.0	0.628

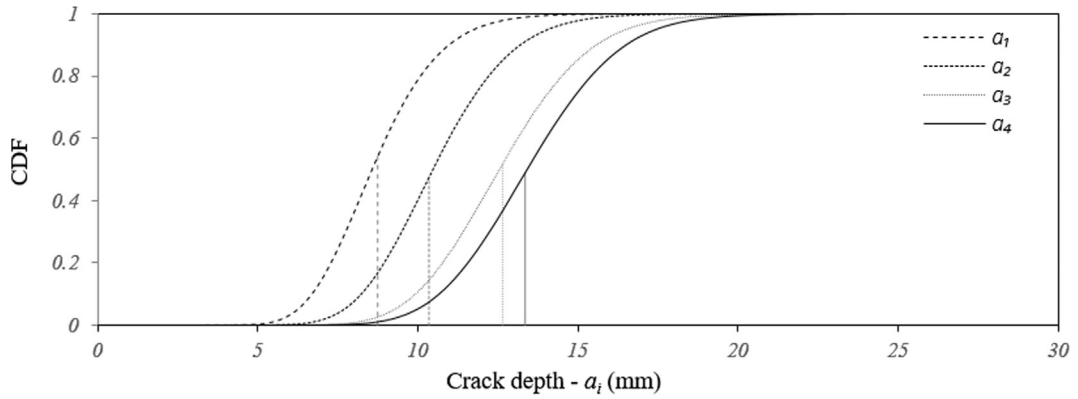

Fig. 10. CDF of crack depths, a_i.

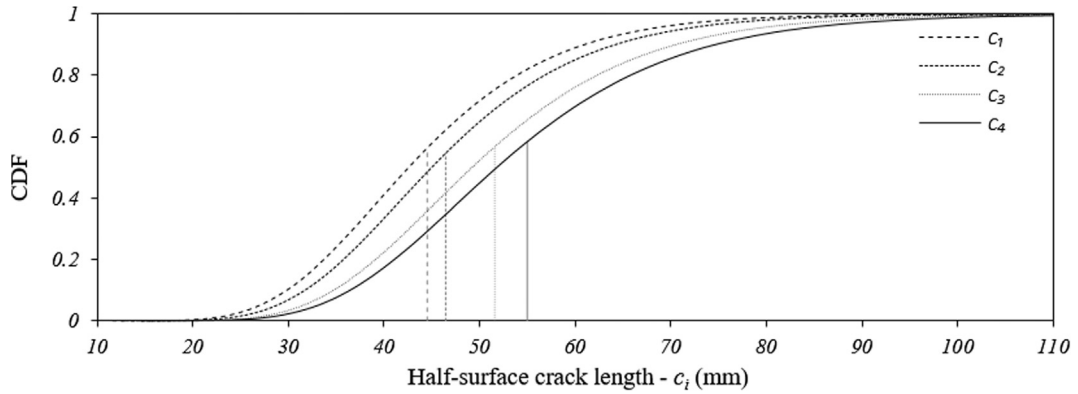

Fig. 11. CDF of half-surface crack lengths, c_i.

$$N_s = \frac{1}{\delta_{P_f}^2}\left(\frac{1-P_f}{P_f}\right) \tag{19}$$

Importance sampling is a corrective sampling method in which the distribution of sampling points concentrated in the region of most importance [32]. Using *Rt* software, the importance sampling is carried out around the Most Probable Point (MPP) from the *FORM* analysis, considering a target δ_{P_f} equal to 0.02.

The outputs obtained from different reliability methods are mentioned in Table 5. Since a large number of samples (approximately of 450,000) generated in *histogram sampling* method; the obtained results are considered as reference data and other results are compared with them. Several inferences can be drawn from these assessments:

Table 5
Probabilities of failure (PoF) obtained by different methods.

Limit state function	Histogram sampling PoF (%)	Probability sampling		Importance sampling		FOSM		FORM		MFORM	
		PoF (%)	Diff.* (%)	PoF (%)	Diff.* (%)	PoF (%)	Diff.* (%)	PoF (%)	Diff.* (%)	PoF (%)	Diff.* (%)
$g_1^a(\boldsymbol{x})$	45.77	45.09	−1.49	44.82	−2.08	53.67	17.26	44.35	−3.10	45.69	−0.17
$g_2^a(\boldsymbol{x})$	52.54	52.23	−0.59	52.33	−0.40	62.00	18.01	49.54	−5.71	60.08	14.35
$g_3^a(\boldsymbol{x})$	48.12	47.64	−1.00	47.69	−0.89	60.13	24.96	44.53	−7.46	49.24	2.33
$g_4^a(\boldsymbol{x})$	51.10	50.16	−1.84	50.96	−0.27	62.93	23.15	47.53	−6.99	55.34	8.30
$g_1^c(\boldsymbol{x})$	43.66	42.64	−2.33	43.10	−1.28	49.53	13.44	43.42	−0.55	43.50	−0.37
$g_2^c(\boldsymbol{x})$	45.39	44.71	−1.50	45.25	−0.31	51.55	13.57	44.18	−2.67	44.70	−1.52
$g_3^c(\boldsymbol{x})$	43.30	42.78	−1.2	43.25	−0.12	50.28	16.12	40.68	−6.05	42.36	−2.17
$g_4^c(\boldsymbol{x})$	41.67	41.25	−1.01	41.47	−0.48	49.14	17.93	38.53	−7.53	36.92	−11.4
$g^L(\boldsymbol{x})$	18.82	18.67	−0.80	18.85	0.16	24.73	31.40	15.69	−16.63	17.79	−5.47

* Difference from histogram sampling (first column) data.

(1) For half-surface crack lengths, c_i, the probabilities of exceedance of experimental results, predicted by *histogram sampling* method are all below fifty percent. For crack depths, a_i, the results are somewhat different. The comparison of these PoFs with deterministic results (Fig. 3) can clarify the importance of uncertainties in prediction of the crack growth after each of four creep-fatigue loadings.
(2) Three sampling methods lead to approximately similar results. Selection of the value of 0.02 for the target CoV of failure probability, δ_{P_f}, in *probability sampling* and *importance sampling* methods, reduces the number of samples, significantly, compared with approximately 450,000 samples used in *histogram sampling* method. In most cases, the results of *importance sampling* approach are more accurate than those obtained by *probability sampling* method. At low and high probabilities of failure, *importance sampling* method has a more effective role in the calculation of probabilities. For example, in prediction of PoF related to creep rupture life's limit state function, $g^L(\boldsymbol{x})$, the number of samples in *histogram sampling*, *probability sampling* and *importance sampling* methods are equal to ~ 450000, 10,894 and 3389, respectively; while the difference between the importance and histogram sampling results is only 0.16%.
(3) *FOSM* (First Order Second Moment) approach has not led to reliable results compared to *histogram sampling* method outputs and therefore this approach is not recommended.
(4) For limit state functions, $g_i^a(\boldsymbol{x})$ and $g_i^c(\boldsymbol{x})$, the difference between FORM and histogram sampling results is at most 7.53%. But this difference is about 16.6% for limit state function, $g^L(\boldsymbol{x})$.

It should be noted that, *MFORM* (Modified FORM) method which performed aimed at improving the predictions, did not necessarily lead to more accurate results compared with *FORM* (e.g. for g_2^a, g_4^a and g_4^c). Therefore, this method should be used more cautiously.

3.4. Sensitivity analysis

Importance measures are an important by-product of *FORM* analysis, which may provide useful information about the order of importance of random variables. If there is a correlation between random variables (such as here), the γ importance vector can be used to investigate the relative importance of the random variables [33]. The elements of γ importance vector represent valuable data:

- The sign of the elements of this vector indicates the nature of the random variables. A positive (negative) value of element, γ_i, shows that the associated random variable, x_i, is of load (capacity) type.
- The magnitude of the elements of γ importance vector, determine the order of importance of the random variables. A greater magnitude of element, γ_i, means that the random variable, x_i, is of more importance.

The order of importance of the random variables, correspond to different limit state functions, summarized in Table 6. In order to understand more clearly, the elements of γ importance vector associated with limit state functions $g_i^a(\boldsymbol{x})$ and $g_i^c(\boldsymbol{x})$, are illustrated in Figs. 12 and 13, respectively.

Figs. 12 and 13 show that, in the calculation of probability of exceedance of experimental crack sizes ($P(g_i^a(\boldsymbol{x}) \leqslant 0)$ and $P(g_i^c(\boldsymbol{x}) \leqslant 0)$), uncertainties in "geometry parameters" and "material behavior" are of more importance, compared with uncertainties

Table 6
γ importance measure of random variables.

Random variable (x_i)	Symbol	γ importance measure								
		$g_1^a(\boldsymbol{x})$	$g_2^a(\boldsymbol{x})$	$g_3^a(\boldsymbol{x})$	$g_4^a(\boldsymbol{x})$	$g_1^c(\boldsymbol{x})$	$g_2^c(\boldsymbol{x})$	$g_3^c(\boldsymbol{x})$	$g_4^c(\boldsymbol{x})$	$g^L(\boldsymbol{x})$
Material behavior										
Creep deformation scaling factor	F_d	0.15	0.24	0.32	0.32	0.01	0.04	0.10	0.12	0.1
Creep crack eq. factor	A	0.10	0.17	0.22	0.23	0.01	0.03	0.07	0.09	0.07
Fatigue crack eq. factor	C_f	0.07	0.27	0.38	0.42	0.01	0.06	0.17	0.23	0.18
Geometry parameters										
Initial crack depth	a_0	0.98	0.89	0.76	0.73	0.72	0.74	0.75	0.75	0.52
Initial aspect ratio	c_0/a_0	0.05	0.15	0.24	0.27	0.70	0.66	0.61	0.58	0.41
Arm length	l	0.02	0.05	0.07	0.08	0	0.01	0.03	0.04	0.14
Plate thickness	t	−0.06	−0.15	−0.19	−0.20	−0.01	−0.04	−0.09	−0.13	−0.46
Plate width	w	−0.04	−0.09	−0.12	−0.13	0	−0.02	−0.05	−0.06	−0.29
Test condition										
Maximum load (fatigue)	L_f	0	0.01	0.02	0.02	0	0	0.01	0.01	0.01
Maximum load (creep-fatigue)	L_{cf}	0.02	0.04	0.05	0.05	0.00	0.01	0.02	0.03	0.13
Load ratio (fatigue)	R_f	0	0	−0.01	−0.01	0	0	0	0	0
Load ratio (creep-fatigue)	R_{cf}	0	−0.01	−0.01	−0.01	0	0	0	−0.01	0
Creep hold time	t_{dwell}	0	0.01	0.01	0.01	0	0	0	0	0
Temperature	θ	0	0	0	0	0	0	0	0	0.43

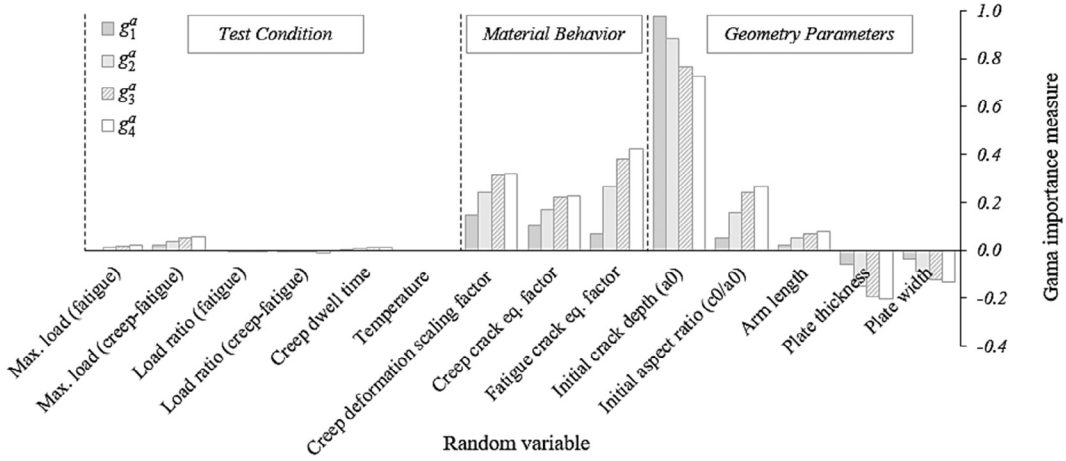

Fig. 12. γ importance measure associated to crack depth limit state functions, $g_i^a(\boldsymbol{x})$.

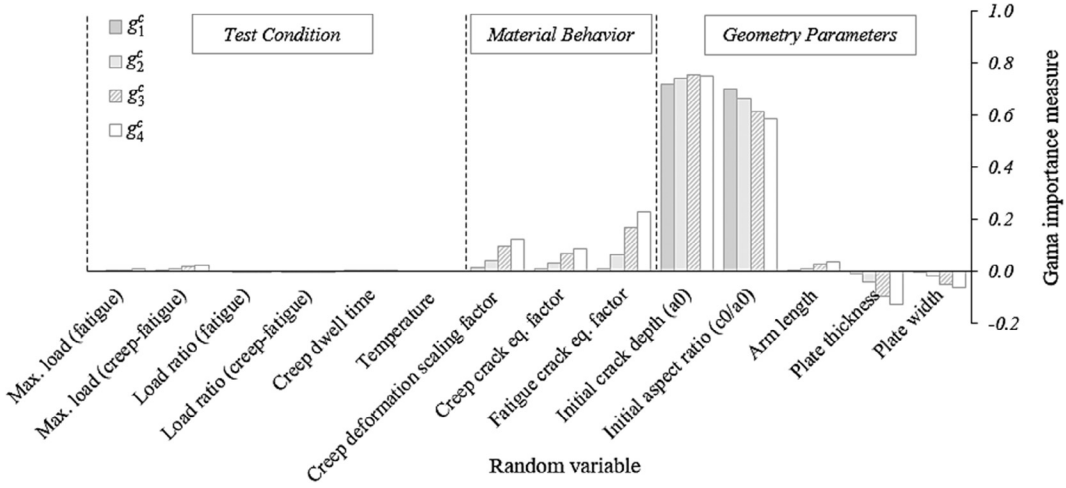

Fig. 13. γ importance measure associated to crack surface limit state functions, $g_i^c(\boldsymbol{x})$.

in "test condition". However, in determination of PoF corresponds to $g^L(\boldsymbol{x})$, some random variables, which fall into "test condition" uncertainties category, i.e. test temperature, θ, and maximum load in creep-fatigue cycles, L_{cf}, become more important.

The variables thickness and width of the plate have negative amount of γ measure and therefore, are of capacity type. For all limit state functions, the variable initial crack depth, a_0, with assumed distribution and CoV of Table 3, has the greatest order of importance. For limit state functions, $g_i^a(\boldsymbol{x})$, by increasing loading cycles from 1st to 4th creep-fatigue loading, the importance of a_0 will be decreased and the importance of almost other variables, will be increased. For limit state functions, $g_i^c(\boldsymbol{x})$, both variables initial crack depth, a_0, and initial aspect ratio, c_0/a_0, have a significant order of importance. However, by increasing loading cycles, the importance of a_0 will not vary, considerably; while the importance of c_0/a_0 will be decreased.

It should be mentioned that, in general, probabilistic assessments and consequently the importance of random variables may be affected by the randomness level of these variables. For example, it can be found that, in this study, the importance of initial crack depth, a_0, and initial aspect ratio, c_0/a_0, are significantly affected by the CoV of these two parameters. Figs. 14 and 15 that are respectively associated to the limit state functions g_4^a and g_4^c, show that the importance of initial crack depth, a_0, and initial aspect ratio, c_0/a_0, will be decreased by decreasing the CoV of these two parameters.

4. Conclusions

The purpose of this study is to investigate the effects of different sources of uncertainty on the prediction of creep-fatigue crack growth, which has been implemented on a known problem. This problem consists of a 316L(N) austenitic stainless steel plate with a semi-elliptical surface crack, subjected to a set of fatigue and creep-fatigue loading conditions [20]. Deterministic calculations as a key component of the probabilistic assessments, were adopted from references [14] and [21]. Deterministic predictions of crack growth at the deepest and surface points (Figs. 3 and 4) show relatively good agreement with the experimental data. However,

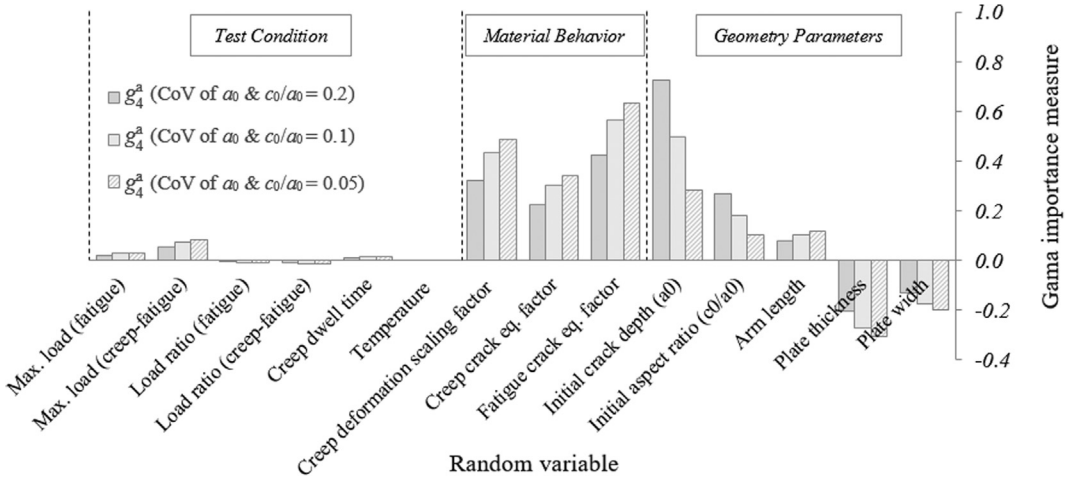

Fig. 14. Effect of CoV variations of initial crack depth, a_0, and initial aspect ratio, c_0/a_0, on γ importance measure, associated to final crack depth limit state function, $g_4^a(\boldsymbol{x})$.

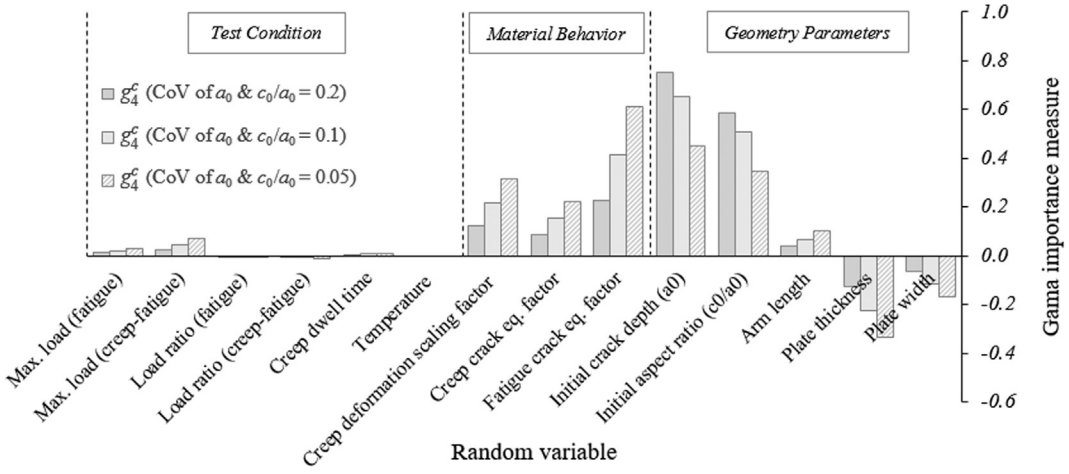

Fig. 15. Effect of CoV variations of initial crack depth, a_0, and initial aspect ratio, c_0/a_0, on γ importance measure, associated to final crack surface limit state function, $g_4^c(\boldsymbol{x})$.

several issues are encountered in these deterministic evaluations which are:

- The solutions of the stress intensity factors [24] and reference stress [26], have been accompanied by assumptions and constraints, that may not be entirely met in the present study.
- The assumptions and details of the deterministic procedure, can be found in [14,21].
- It should be noted that the employed approach, is not necessarily applicable to other creep-fatigue problems. For each creep-fatigue crack growth problem, it may be possible to use the existing well-known procedures such as those given in [21,22].

Probabilistic assessments have been carried out in three areas: (I) estimation of probability distribution of desired outputs (e.g. propagated crack sizes), (II) calculation of probabilities of exceedance of experimental results, and (III) sensitivity analysis. In the first area, it has been shown that, the prediction of the last propagated crack size, a_4 and c_4, is associated with more uncertainty (more standard deviation), compared to the first propagated crack sizes, a_1 and c_1 (Figs. 5 and 6). It has been also illustrated that, the uncertainty in the prediction of the half-surface crack lengths, c_i, is significantly more than the crack depths, a_i (Fig. 7). The second area focuses on the implementation of different reliability methods to determine the probabilities of exceedance of experimental data, which are reported by Poussard and Moulin [20]. These evaluations clarified the importance of consideration of uncertainties in creep-fatigue crack growth prediction, in comparison with the deterministic approach. Furthermore, it has been found that, the *importance sampling* method might be an efficient and almost accurate approach in the determination of probabilities of failure. In the last area, sensitivity analysis was performed in order to investigate the importance of random variables related to different limit state functions (Eqs. (16)-(18)). It is shown that the initial crack depth, a_0, with the assumed distribution of Table 3, has the greatest value of γ importance measure in all of the limit state functions. Initial aspect ratio, c_0/a_0, is another important random variable, in the

prediction of probabilities of exceedance of experimental crack surface lengths (related to limit state functions, g_i^c). Figs. 14 and 15 showed that variation in the CoV of the initial crack size, a_0 and c_0/a_0 can significantly change the importance of these parameters. In determination of PoF corresponds to $g^L(\boldsymbol{x})$, test temperature, θ, and maximum load in creep-fatigue cycles, L_{cf}, become more important. Some issues related to the probabilistic assessments, are as follows.

- There are several sources of uncertainties, such as "models' uncertainty" and "experiment results", that are not investigated in this study. Furthermore, various parameters in stress intensity factor equations [24], creep rupture life (Eq. (15)), etc. are considered as constant values (not random variables).
- In this study, the uncertainties in "test condition" (see Table 3), are assumed as unique values for the entire test, not for each cycle, individually. Although, this assumption may be not consistent with actual state of practical problems, but this can be implemented in such probabilistic assessments and sensitivity analysis.
- The importance of random variables indicates which variable can be ignored in probabilistic assessments (i.e. considered as constant value), and which one(s) is needed to be considered more precisely.
- It is necessary to take into account the correlation between random variables in probabilistic evaluations, consistent with the available data. However, in the present study, because of the convergence problems in Newton algorithm within the Nataf transmission, the negative correlation between creep strain rate scaling factor, F_d, and constant A in creep crack growth rate equation, could not have any high value. Furthermore, the same scaling factor, F_d, is assumed for both primary and secondary creep (Eq. (10)).

References

[1] Li W, Yang X, Zhang G, Ma Y. Cohesive zone modeling of creep–fatigue crack propagation with dwell time. Adv Mech Eng 2017;9.
[2] Liu H, Bao R, Zhang J, Fei B. A creep–fatigue crack growth model containing temperature and interactive effects. Int J Fatigue 2014;59:34–42.
[3] Mehmanparast A, Davies C, Nikbin K. Evaluation of the testing and analysis methods in ASTM E2760-10 creep-fatigue crack growth testing standard for a range of steels. Creep-Fatigue Interact: Test Meth Models: ASTM Int 2011.
[4] Nikbin K. Creep/fatigue crack growth testing, modelling and component life assessment of welds. Strength Fract Complex 2015;9:15–29.
[5] Saxena A. Creep and creep–fatigue crack growth. Int J Fract 2015;191:31–51.
[6] Xu L, Zhao L, Gao Z, Han Y. A novel creep–fatigue interaction damage model with the stress effect to simulate the creep–fatigue crack growth behavior. Int J Mech Sci 2017;130:143–53.
[7] Mao H, Mahadevan S. Reliability analysis of creep–fatigue failure. Int J Fatigue 2000;22:789–97.
[8] Harlow D, Delph T. A probabilistic model for creep-fatigue failure. J Pressure Vessel Technol 1997;119:45–51.
[9] Ibisoglu F, Modarres M. Probabilistic life models for steel structures subject to creep fatigue damage. Int J Prognost Health Manage 2015.
[10] Hu D, Ma Q, Shang L, Gao Y, Wang R. Creep-fatigue behavior of turbine disc of superalloy GH720Li at 650 C and probabilistic creep-fatigue modeling. Mater Sci Engng A 2016;670:17–25.
[11] Dogan B, Ceyhan U, Korous J, Mueller F, Ainsworth R. Sources of scatter in creep/fatigue crack growth testing and their impact on plant assessment. Weld World 2007;51:35–46.
[12] Wei Z, Yang F, Cheng H, Nikbin K. Probabilistic prediction of crack growth based on creep/fatigue damage accumulation mechanism. J ASTM Int 2011;8:1–15.
[13] Wei Z, Yang F, Lin B, Luo L, Konson D, Nikbin K. Deterministic and probabilistic creep–fatigue–oxidation crack growth modeling. Probab Engng Mech 2013;33:126–34.
[14] Baker A, O'Donnell M, Dean D. Use of the R5 Volume 4/5 procedures to assess creep–fatigue crack growth in a 316L (N) cracked plate at 650° C. Int J Press Vessels Pip 2003;80:481–8.
[15] Chapuliot S, Drubay B, Lacire-Papin M, Poette C, Deschanels H, Martelet B. A French guideline for defect assessment and leak before break analysis. Mater High Temp 1998;15:303–12.
[16] Curtit F, Laiarinandrasana L, Drubrav B, Martelet B. Creep fatigue crack growth of semielliptical defect in austenitic stainless steel plates. ECF12, Sheffield; 1998.
[17] Curtit F, Piques R, Chapuliot S, Cambefort P. Propagation de fissures semi elliptiques en fatigue-fluage dans des plaques d'acier 316L (N) sollicitées en flexion à 650° C. Le Journal de Physique IV 2000;10:Pr4-305-Pr4-10.
[18] Marie S, Delaval C. Fatigue and creep–fatigue crack growth in 316 stainless steel cracked plates at 650° C. Int J Press Vessels Pip 2001;78:847–57.
[19] Poussard C, Celard N, Drubay B, Moulin D. Creep-fatigue crack growth in austenitic stainless steel centre cracked plates at 650° C. Part II: Defect assessment according to the A16 document. Mater High Temp 1998;15:313–21.
[20] Poussard C, Moulin D. Creep-fatigue crack growth in austenitic stainless steel centre cracked plates at 650° C. Part I: experimental study and interpretation. Mater High Temp 1998;15:87–94.
[21] R5. Assessment. Procedure for the high temperature response of structures. EDF Energy 2012.
[22] A16. Guide for Leak Before Break Analysis and Defect Assessment. AFCEN; 2007.
[23] Park C-G, Kim J-B, Lee J-H. A comparison study of creep-fatigue defect growth evaluations for a SFR IHTS piping. J Power Energy Syst 2008;2:20–8.
[24] Newman Jr J, Raju I. An empirical stress-intensity factor equation for the surface crack. Eng Fract Mech 1981;15:185–92.
[25] BS7910. Guide to Methods for Assessing the Acceptability of Flaws in Metallic Structures. BSI; 2013.
[26] Goodall I, Webster G. Theoretical determination of reference stress for partially penetrating flaws in plates. Int J Press Vessels Pip 2001;78:687–95.
[27] Harris D. Probabilistic fracture mechanics. Probabilistic structural mechanics handbook. Springer; 1995. p. 106–45.
[28] R6. Assessment for the Integrity of Structures Containing Defects Revision 3: British Energy; 1998.
[29] Chevalier M, Smith D, Dean D. The reliability of structural systems operating at high temperature: replacing engineering judgement with operational experience. Int J Press Vessels Pip 2012;98:65–75.
[30] JCSS Probabilistic Model Code, Part 3: Resistance models. Joint Committee on Structural Safety (JCSS); 2011.
[31] Mahsuli M, Haukaas T. Computer program for multimodel reliability and optimization analysis. J Comput Civil Eng 2012;27:87–98.
[32] Haldar A, Mahadevan S. Probability, reliability, and statistical methods in engineering design. John Wiley; 2000.
[33] Der Kiureghian A. First-and second-order reliability methods. Engineering design reliability handbook; 2005:14.

Probabilistic assessment of creep-fatigue crack propagation in austenitic stainless steel cracked plates

Vojdani, A.

2018-07-20

Vojdani A, Farrahi GH, Mehmanparast A, Wang B. (2018) Probabilistic assessment of creep-fatigue crack propagation in austenitic stainless steel cracked plates. Engineering Fracture Mechanics, Volume 200, September 2018, pp.50-63

https://doi.org/10.1016/j.engfracmech.2018.07.022